行政院國家科學委員會專題研究計畫　期中進度報告

應用於數位電視之低功率基頻接收器(1/3)

計畫類別：個別型計畫
計畫編號：NSC94-2215-E-009-044-
執行期間：94 年 08 月 01 日至 95 年 07 月 31 日
執行單位：國立交通大學電子工程學系及電子研究所

計畫主持人：李鎮宜

報告類型：精簡報告
報告附件：出席國際會議研究心得報告及發表論文
處理方式：本計畫可公開查詢

中　華　民　國 95 年 6 月 1 日

行政院國家科學委員會補助專題研究計畫期中成果報告

應用於數位電視之低功率基頻接收器(1/3)

計畫類別：個別型計畫

計畫編號：NSC94-2215-E009-044-

執行期間：94 年 8 月 1 日 至 95 年 7 月 31 日

計畫主持人：李鎮宜

計畫參與人員：劉軒宇、游瑞元、劉子明、侯康正、黃毅宏、楊俊彥、曹堉琪、李文平、林大嘉

執行單位：國立交通大學電子工程系所

中 華 民 國 95 年 5 月 28 日

中文摘要

此期中報告主要針對 DVB-T/H 基頻接收器系統的時間同步、通道等化模組做客制化設計與研究。繼承前一期計畫之研究成果，單一晶片化設計之 DVB-T/H 基頻接收器得以實現，目前針對各功能模組效能、架構以及功率消耗等項目進行改進。本報告第一部份，我們研究改進前一測試晶片中時間同步系統的運算時程，藉以符合 DVB-H burst operation 條件下的時間限制，並針對取樣時脈偏差追蹤機制(SCO tracking)提出更新的架構。第二部分則是著重在 Frequency Selected Fading Channel 跟 Doppler Effect 結合效應下，研究適當的演算方法，以克服在真實時變多通道環境下通道等化功能的挑戰。

關鍵字：數位視訊系統、同步系統、時變多通道環境等化器

Abstract:

In this report, we study and customize the framing synchronization, channel equalization modules for DVB-T/H baseband receiver. Based on previous NSC supporting project, a single test chip for DVB-T/H baseband receiver was implemented. The focusing tasks of current state is improving, refining the performance, architecture, and power consuming for key modules. In the first part, we study the architecture of previous test chip and try to improve the latency of system synchronization procedures for timing requirement of DVB-H burst operation. Also, we propose new architecture for SCO tracking. The second part is estimation algorithm refining for Frequency Selected Fading Channel with Doppler effect. We study some methods that should overcome the time-variance multipath channel.

Keywords: DVB-T baseband receiver, synchronization system, time. Channel estimation for time-variance multipath channel.

Part I

Reduction of Synchronization Time and Proposed SCO tracking Architecture for DVB-T/H System

I. Introduction

Orthogonal frequency division multiplexing (OFDM) modulation offers a good solution for high rate wireless data transmission and is also very efficient in spectrum utilization. It is well known that OFDM in wireless communication system like digital video broadcasting-terrestrial (DVB-T) [1] system must be against fast frequency selective fading channel and is sensitive to timing and frequency synchronization errors, which cause inter-carrier interference (ICI), inter-symbol interference (ISI), carrier frequency offset (CFO), sampling clock offset (SCO) and degrades system performance. Figure 1 showing Timing-Slicing technology in DVB-H system [1], provides a low power consumption methodology. The saving of power consumption depends on each kind of parameter in Time Slice identifier descriptor in DVB-data [2]. And we can check the related details of these parameters and the formulas of power consumption saving.

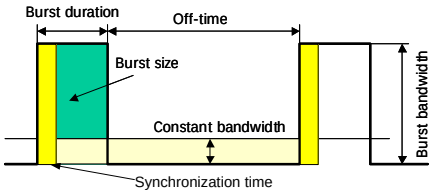

Fig. 1: Timing-Slicing technology in DVB-H system

In Time Slice methodology, we know that the synchronization time dominate the saving of power consumption. Fig.2 shows the composition of synchronization time. We can get the information Synchronization Time equals (Acquisition Time + TPS decode Time + RS packet synchronization Time) or (Acquisition Time + Tracking Time). And the determination of Synchronization Time depends on which is longer. Acquisition Time is about 10 symbols, TPS decode Time is about 2 frames (136 symbols), and RS sync. Time is about 4/2/1 frames (272/136/68 symbols) in 8k/4k/2k mode in conventional method. However Tracking Time depends on the channel influence, and it has no fixed value. Thus we can consider that reduction of acquisition time, TPS decoded time, RS packet synchronization time and Tracking Time can clearly reduce Synchronization Time and increase the saving of power consumption. And the tracking time is the faster the better.

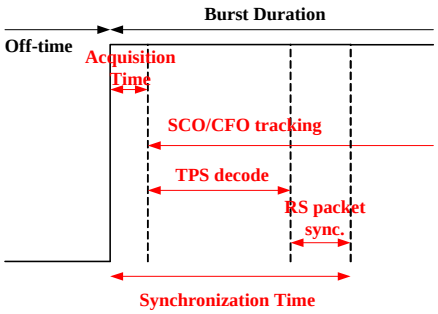

Fig.2: the composition of synchronization time

In this report, two topics would be introduced: one is reduction of TPS decode Time and RS packet synchronization Time; the other topic is improvement of SCO tracking and estimation. SCO would accumulate in Fig. 3 and Fig. 4 that SCO increases linearly in time domain causes two-order phase rotation increasing symbol by symbol. The relation between the phase difference and SCO can be represented as:

$$\varphi_l(k) - \varphi_{l-1}(k) \approx 2\pi\Delta f\,(N_g + N)T + \frac{2\pi(N_g + N)k\zeta}{N}$$

Where ζ is SCO, N_g means guard interval length, N means 2/4/8k, l is symbol index and k is carrier index.

The reduction of TPS decoding Time and RS packet synchronization time, will be introduce in section 2. In the

other side, the improvement of SCO tracking and estimation will be introduced in section 3. The simulation and comparison will be introduced in section 4. We make some conclusion in section 5.

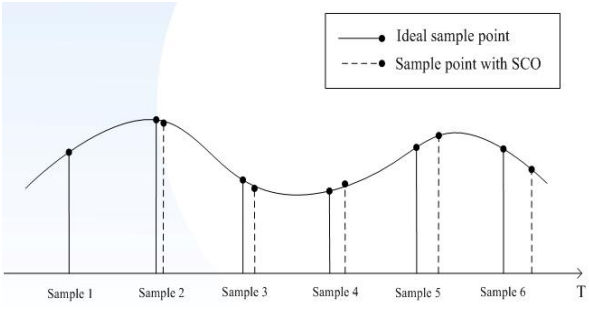

Fig. 3: Impact of sampling clock offset in time domain

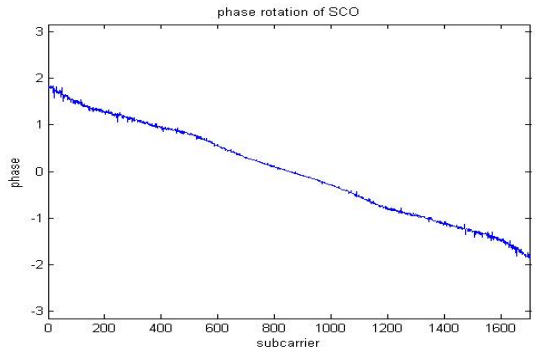

Fig. 4: Impact of sampling clock offset in frequency domain

II. The Reduction of TPS Decoding Time and RS Packet Synchronization time

The block diagrams of inner and outer receiver are shown in Fig. 5. The marked parts are the decision blocks of TPS decoded time and RS packet synchronization time.

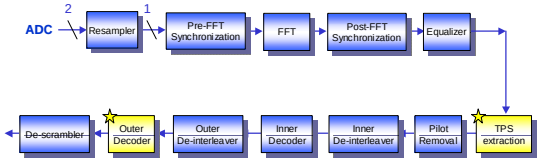

Fig. 5: block diagrams of inner and outer receiver

II.1.The Reduction of TPS Decoding Time

The structure of TPS listed in DVB-T/H standard [1] is composite of 68 words (one frame) and concludes 17 synchronization words. The conventional design [4] of TPS decoded costs 135 (68 + 67) symbols time in the worst situation to receive the completed TPS word and then synchronizes the header. The proposed method is to buffer the previous 68 words. When finding the 17 synchronization words, we read the previous 51 words information as TPS decoded words. And the worst case of the decoded time is 85 (68+17) symbols. We can see the impact in Fig. 6.

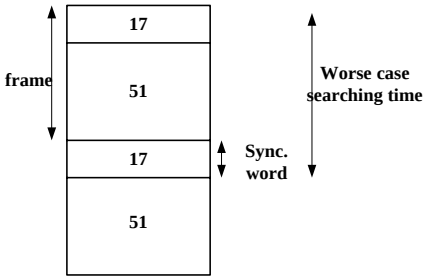

Fig. 6: impact of proposed TPS decoded word

II.2.The Reduction of RS Packet Synchronization Time

As Fig. 5 shown, we know the outer decoder is RS decoder. And the input of RS decoder must be a completed packet. In other word, we must synchronize the header of the RS packet. The impact of RS packet is shown as Fig. 7.

Fig. 7: the impact of the RS packet

The worst condition of RS packet synchronization time in conventional method is 272/136/68 symbols in 2k/4k/8k mode. The conventional method is to synchronize the packet in frames, but the proposed method just needs to calculate the carrier index to synchronize the packet in the carriers. The proposed method will help us to reduce the synchronization time a lot. We can reduce the synchronization time to 5/3/2 symbols (be larger than 6528 carriers).

III. The Improvement of SCO Tracking and Estimation

This section introduces proposed SCO tracking architecture and proposed SCO estimation algorithm both. The proposed tracking architecture and tracking algorithm

provide different improvement. The proposed tracking architecture reduces the time tracking to acceptable range and the proposed estimation algorithm improves the estimation accuracy.

III.1. Proposed SCO Estimation Algorithm

The first conventional SCO estimation algorithm is mentioned [5], and it is a method of jointed SCO and CFO estimation (CFD/SFD) by calculating the phase difference between continual pilots of two consecutive symbols and then do average to the left part and right part and calculate. The method has low mean error but unavoidable variance of SCO estimation. Then the linear least square is published [7]. Combine these two different method, we obtain a jointed SCO and CFO LLS estimation method [3]. The principle of the method is to calculate the phase difference between continual pilots of two consecutive symbols and then multiply a linear weight. Finally, calculate the slope of the line. The equations are listed as:

$$\hat{\zeta} = \frac{1}{2\pi\left(1+N_g/N\right)} \cdot \sum_{k=-M/2}^{M/2-1} B_{2,k} \cdot y_{l,k} \quad ,$$

$$y_{l,k} = Arg\left[z_{l,k} \cdot z_{l-1,k}^{*}\right]$$

$$B = (A^T A)^{-1} A^T$$

$$A = \begin{bmatrix} 1 & k_1 \\ 1 & k_2 \\ \vdots & \vdots \\ 1 & k_M \end{bmatrix} \mid k_i \in CP$$

Where $\hat{\zeta}$ is estimated SCO, N_g means guard interval length, N means 2/4/8k, $z_{l,k}$ is carrier data, l is symbol index, k is continual pilot index, M is numerous of continual pilots in a symbol, $y_{l,k}$ is the phase difference between continual pilots of two consecutive symbols, and B is the linearization matrix. The architecture of jointed SCO/CFO LLS estimation is shown in Fig. 8.

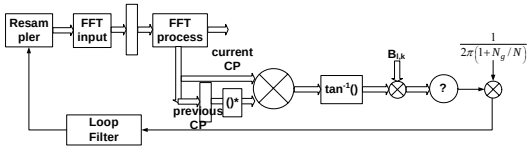

Fig. 8: impact of SCO estimation architecture

The proposed SCO estimation method has a key difference between the conventional designs: using the scatter pilots to replace the continual pilots. The equations become:

$$\hat{\zeta} = \frac{1}{2\pi\left(1+N_g/N\right)\cdot 4} \cdot \sum_{k=-N/2}^{N/2-1} B_{2,x} \cdot y_{w,x} \quad ,$$

$$y_{w,x} = Arg\left[z_{w,x} \cdot z_{w-1,x}^{*}\right]$$

$$D = (C^T C)^{-1} C^T$$

$$C = \begin{bmatrix} 1 & x_1 \\ 1 & x_2 \\ \vdots & \vdots \\ 1 & x_N \end{bmatrix} \mid x_i \in SP$$

Where z is carrier data, w is symbol index, x is scatter pilot index, N is numerous of scatter pilots in a symbol, y is the phase difference between scatter pilots of 4 symbol distance location, and D is the linearization matrix. The advantage is obvious, because the numerous of scatter pilots is 142/284/568 in 2/4/8k mode but the numerous of continual pilots is 45/89/177 in 2/4/8k mode. The architecture of proposed SCO estimation is shown in Fig. 9.

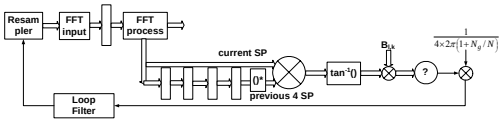

Fig. 9: impact of proposed SCO estimation architecture.

Hence the proposed scatter pilot method is more accurate than continual pilots method. And the disadvantage of proposed method is the additional 4 buffers and throughput of estimation outcome up to 5 symbols. The buffers have already existed in 2-D channel estimation methodology [4] and the problem of throughput of estimation outcome will be solved in followed contents. We can also see the simulation results in section 4.

III.2. Conventional SCO Tracking Architecture

To compare these differences between different architecture, we choose the same algorithms: the linear least square method [3]. And the selection of algorithm will not affect the comparison of difference architecture. According to Fig. 8, we can plot the timing diagram in Fig. 10. In which d means the estimation outcome after loop filter and the number in timing diagrams means symbol

index. And the same color means the same resample-modified symbol, in other words, the same color means the same effect of SCO.

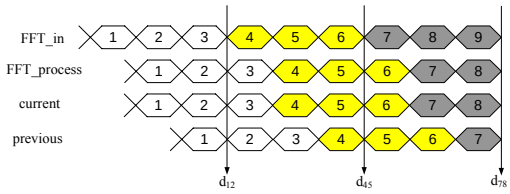

Fig. 10: Timing diagram of conventional SCO tracking architecture

Because of the FFT process latency, after calculating the phase difference between continual pilots of consecutive symbols, the feedback outcome passes to time domain and then waits two symbols time and calculate next SCO in third symbol. Thus, the throughput is three symbols.

III.3. Proposed SCO Tracking Architecture: Feedback Forward method

The principle of proposed SCO tracking architecture is to add a feedback forward path in the SCO estimation loop. It is shown as Fig. 11. The feedback forward architecture is to extract the previous two SCO estimation values after loop filter and then through some simple transformation execution, the estimation values would change to become the phase information. Finally, do the phase compensation to the phase difference between continual pilots of two f-domain symbols that were not resample-modified at t-domain. As we compensate the phase forward, we would not wait for the FFT process latency, and we will improve the throughput of SCO tracking outcome. The timing diagram is shown in Fig. 12. Like the conventional design, the same color means the same resample-modified symbol, in other words, the same color means the same effect of SCO. We can obviously see the f-domain symbol is modified. The throughput becomes one symbol. The phase compensated equation is:

$$\varphi(k) = 2\pi(1 + N_g / N)k \times d$$

Where d means the estimated outcome of SCO after loop filter, $\varphi(k)$ means the phase compensation, and k means continual pilot index.

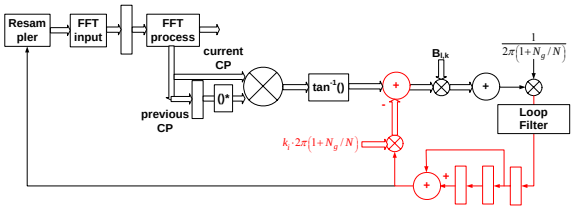

Fig. 11: impact of proposed SCO tracking architecture

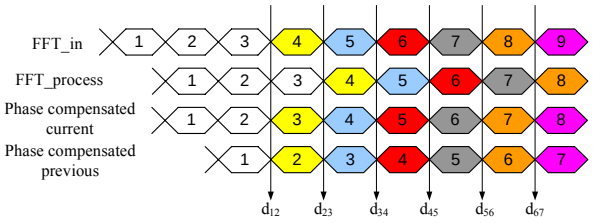

Fig. 12: timing diagram of proposed SCO tracking architecture

Now, we choose proposed SCO estimation algorithm, scatter pilot method, to replace the conventional algorithm. The architecture is shown in Fig. 13, and the timing diagram is shown in Fig. 14. The phase compensation equation is:

$$\varphi(k) = 2\pi(1 + N_g / N) \cdot 4k \times d$$

Where d means the estimated outcome of SCO after loop filter, $\varphi(k)$ means the phase compensation, and k means scatter pilot index. In section 3.1, we mentioned about the problem of the throughput of SP method. The throughput of the estimation outcome is high to six symbols, and five symbols for waiting for the scatter pilot location and one symbol for FFT process. In this section we will no longer see the problem because of the feedback forward path. The feedback forward path can add in any kind of algorithm and also can solve some problem like low throughput. Hence, this proposed architecture can combine with all other estimation algorithms.

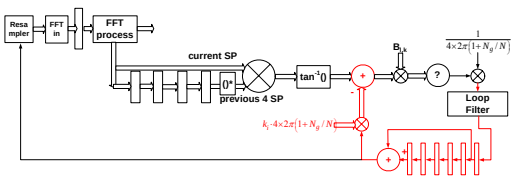

Fig. 13: impact of proposed SCO tracking architecture with SP method

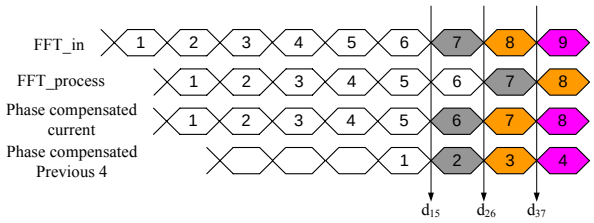

Fig. 14: timing diagram of proposed SCO tracking architecture with SP method

IV. Simulation Result and Comparison

The accuracy of the proposed method would not reduce but the synchronization time definitely reduces. The synchronization time of TPS decode costs from 135 to 85 symbols. And RS packet synchronization time is from 272/136/68 symbols to 5/3/2 in 2k/4k/8k mode. One solution of the synchronization time is (acquisition time + TPS decoded time +RS packet synchronization time). The total results of this proposed system design improve the synchronization time from 417/281/213 to 100/98/97 symbols. Table 1 shows the synchronization time (ms) in 8MHz, 7MHz, 6MHz and 5MHz channel.

Table 1: Synchronization time (ms) in supporting channel

8 MHz	2k mode				4k mode				8k mode			
GI	1/4	1/8	1/16	1/32	1/4	1/8	1/16	1/32	1/4	1/8	1/16	1/32
Conventional	116.8	105.1	99.2	96.3	157.4	141.6	133.8	129.8	238.6	214.7	202.8	196.8
Proposed	28	25.2	23.8	23.1	54.9	49.4	46.7	45.3	108.8	99.8	92.3	89.6
7 MHz	2k mode				4k mode				8k mode			
GI	1/4	1/8	1/16	1/32	1/4	1/8	1/16	1/32	1/4	1/8	1/16	1/32
Conventional	133.4	120.1	113.4	110.1	179.8	161.9	152.9	148.4	272.6	245.4	231.7	224.9
Proposed	32	28.8	27.2	26.4	62.7	56.5	53.3	51.7	124.2	111.7	105.5	102.4
6 MHz	2k mode				4k mode				8k mode			
GI	1/4	1/8	1/16	1/32	1/4	1/8	1/16	1/32	1/4	1/8	1/16	1/32
Conventional	155.7	140.1	132.3	128.4	209.8	188.8	178.3	173.1	318.1	286.3	270.3	262.4
Proposed	37.3	33.6	31.7	30.8	73.2	65.7	62.2	60.4	144.8	130.4	123.1	119.5
5 MHz	2k mode				4k mode				8k mode			
GI	1/4	1/8	1/16	1/32	1/4	1/8	1/16	1/32	1/4	1/8	1/16	1/32
Conventional	186.8	168.1	158.8	154.1	251.8	226.6	214	207.7	381.7	343.5	324.4	314.9
Proposed	44.8	40.3	38.1	36.9	87.8	79	74.7	72.4	173.8	156.4	147.8	143.4

We can see the different synchronization time in different transmission mode, and then we can choose one couple of them to calculate the saving of power consumption. For instance, in 5MHz channel, 4k mode and GI 1/4, the conventional method costs 251.8ms and proposed method costs 87.8ms. According to the reference [2], let Burst Duration be 200ms, Delta-t Jitter be 10ms Constant Bandwidth be 512kbps Burst Size be 1024kbits. Thus, we can obtain the conventional saving of power consumption is 78%, and the proposed method obtains 86% power saving.

We show the comparisons between different algorithms. As mentioned in 3.1, reference [3] proposed a “CP-LLS algorithm” to use the linear least square method between continual pilots of consecutive symbols. Reference [5] mentioned “CP-CFD/SFD algorithm” to joint CFO and SCO tracking, and “CP” means continual pilots too. Table 2 lists the estimation accuracy of the above two algorithm and proposed “SP-LLS algorithm”.

Table 2: the estimation accuracy of the SCO in ppm

	Gaussian		Ricean + Doppler spread 70 Hz		Rayleigh + Doppler spread 70 Hz	
Estimation algorithm	Mean error	Standard deviation	Mean error	Standard deviation	Mean error	Standard deviation
CP-CFD/SFD [5]	0.0694	5.9905	1.3678	7.2908	-2.0967	8.2107
CP-LLS [3]	-0.1567	5.4948	-0.0450	6.3277	-4.0990	8.6082
Proposed SP-LLS	0.0475	1.0645	0.1032	1.3617	-3.5122	4.8212

Thus, we can obviously see the proposed algorithm with best standard deviation and the mean error of proposed SP-LLS is about the same with others. The other simulation result is to show the throughput improvement of the proposed architecture. We compare four different architecture and algorithm collection. First, “CP-LLS conventional architecture” is the conventional architecture that the throughput is 3 symbols time. Second, “CP-LLS feedback forward architecture” is the continual pilot based estimation method with proposed feedback forward

architecture. Then third and fourth, “SP-LLS conventional architecture” and “SP-LLS feedback forward architecture”. The simulation environment is the same. It is in 2k mode, GI equals to 1/4, and adding 20ppm SCO initial value in the Ricean channel with AWGN SNR 15dB. And the loop filter is the function of $K_P + K_I \frac{Z^{-1}}{1-Z^{-1}}$, where $K_I \simeq K_P$ and we take $K_P = 1/8$ in those different conditions. We can see the residual SCO (ppm) in Fig. 15, 16 and 17. Fig. 15 shows the comparison between “CP-LLS with feedback forward” and “CP-LLS”. Fig. 16 shows the comparison between “SP-LLS with feedback forward” and “SP-LLS”. Fig. 17 shows the comparison between “CP-LLS with feedback forward” and “SP-LLS with feedback forward”.

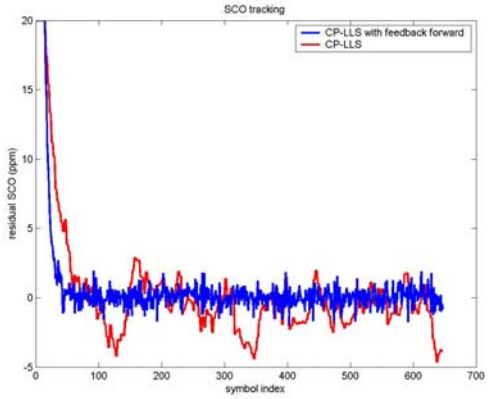

Fig. 15: impact of the residual SCO convergence in CP-LLS algorithm between w/wo feedback forward architecture

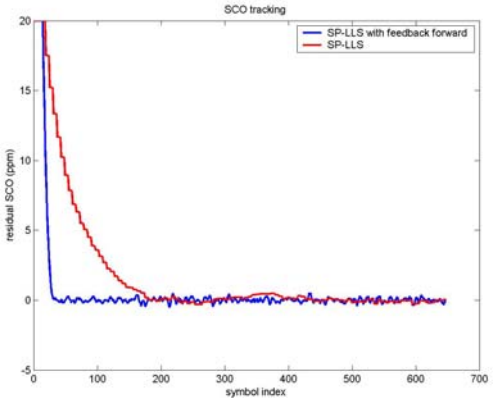

Fig. 16: impact of the residual SCO convergence in SP-LLS algorithm between w/wo feedback forward architecture

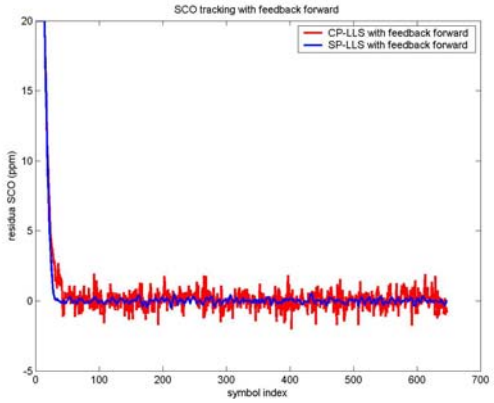

Fig. 17: impact of the residual SCO convergence between CP-LLS and SP-LLS algorithm with feedback forward architecture

The numerous of scatter pilots is more than continual pilots, hence the estimation accuracy of SP method is better than CP method and the feedback forward architecture has higher throughput to let the residual SCO nearby zero ppm more fast, it means to be convergent earlier and also means synchronization time to be reduced. The feedback forward architecture has an additional advantage of estimation. It is a phase compensation method and will also let the phase error compensating to the mean phase regression more closely. We calculate the standard deviation of “SP-LLS feedback forward”, “SP-LLS”, “CP-LLS feedback forward” and “CP-LLS” from 200th to 648th symbol, and they are 0.16468, 0.18906, 0.65816 and 1.37996. We can see the “SP-LLS feedback forward” has the least standard deviation and performs best in the four conditions. Also we can see the convergent symbol of feedback forward architecture is earlier than conventional architecture up to least 125 symbols in SP-LLS method and 50 symbols in CP-LLS method.

V. Conclusion

The synchronization time is reduced by improving TPS decode and RS packet synchronization directly in section II. In section III, improving SCO tracking time, is also helpful for synchronization time. Thus, we can consider the saving of power consumption is increased.

However, section III is pointed on the optimization of the SCO tracking design, and in the future work we can combine the CFO tracking, SCO tracking and fine symbol tracking design into a synchronization tracking design. Further more, we can combine tracking design and acquisition design into a DVB-T/H synchronizer to obtain the most reused hardware and optimized solution.

Part II

Pilot-Symbol-Aided Channel Estimation and Equalizer for DVB-T System

I. Introduction

In wireless communications, the receiver system have to compensate the channel effects including Rayleigh fading, Doppler frequency shift, and additive white Gaussian noise (AWGN). Pilot-symbol-aided channel estimation of time and/or frequency selective channels is another potential application. The basic principle of 1-D pilot-symbol-aided channel estimation is to multiplex pilot symbols known to the receiver into the data stream. Hence, the receiver is able to estimate the process (the channel) at any time given the observations at the pilot locations, assuming the pilot density is sufficient w.r.t. the channel bandwidth. The way the scattered pilots are arranged calls for channel estimation via interpolation. By making use of the (known) pilots, samples $\hat{H}_{l,k} = z_{l,k} / p_{l,k}$ of the channel transfer function (CTF) are obtained. Final estimates $\tilde{H}_{l,k}$ CFR are generated by interpolation in time and frequency direction. In this report, we investigate channel estimation by different interpolation methods. The rest of this report is organized as follows. In section 2, we propose the algorithm of channel estimation including three parts. In Section 3, provides the conclusions.

II. Channel Estimation

In this section, we assume that the channel is time variant. Therefore, the channel frequency response (CFR) for present symbol should be obtained independently. The proposed channel estimation method based on pilot signals and transform domain processing is depicted in Fig. 18.

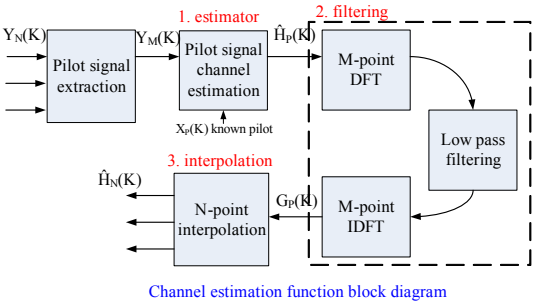

Fig. 18: Channel estimation function block diagram

Here we will focus on these three parts. First, the estimator can get the CFR at pilot location, and second, filtering can reduce the noise effect. Finally, we can get the CFR of whole symbol by interpolation methods. The three key points will be discussed in following.

1. Estimator

When we receive the receiving data $Y_N(K)$, we will extract the pilot signal $Y_M(K)$. The first key point is to get the CFR at pilot location $H_P(K)$ by $Y_M(K)$ and known pilot data $X_P(K)$. We can use LS estimator directly by $\hat{H}_p(k) = Y_M(k) / X_p(k)$. However , this estimator will be easily effected by noise. In fact, in most slowly variant channel environment, this estimator can get improvement. We propose an adaptive filter which can get better performance in slowly variant channel. In this case, the noise can be averaged out from $\hat{H}_p(k)$ by using following adaptive algorithm. The formulation is following.

$$\tilde{H}_{l+1,k} = (1-\beta)\tilde{H}_{l+1,k} + \beta\hat{H}_{l,k} = (1-\beta)Y_{l+1,k} / X_{l+1,k} + \beta\tilde{H}_{l,k}, \beta \in [0,1]$$

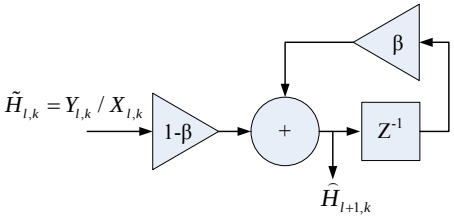

Fig. 19: the diagram of adaptive algorithm

Furthermore, we propose an algorithm to detect the channel changing degree to decide the value of β. Furthermore, the channel is more time dependent as the β lager. When β convergence to 0 which means the channel varying too much over the previous estimator. Because of the standard, the scatter pilots is four symbols a cycle.

The performances in Rayleigh and Ricean channel with different Doppler effects are shown in Fig. 20 and Fig. 21. We can find the channel changing faster as Doppler frequency increasing, and the β of the best performance is decreasing from 0.75 to 0. The CFR of Rayleigh channel is most complicated, so when Doppler increasing to 10 Hz the β is convergence to 0. However, in the fix Rayleigh channel the proposed method can still gain almost 0.7 dB than original design. In Ricean channel, we can see the relationship between β and Doppler effects. The β of best performance is 0.75 at 10Hz, 0.25 at 30Hz, and β is 0 at 70Hz. The proposed method can get better performance in the slow fading channel.

The threshold of β is decided by the adjacent symbol at continuous pilot location. There are many sections in one CFR, and the β will be different in each section. This work is still going. The basic concept, we will use the variance when SNR at QEF to set the decision threshold.

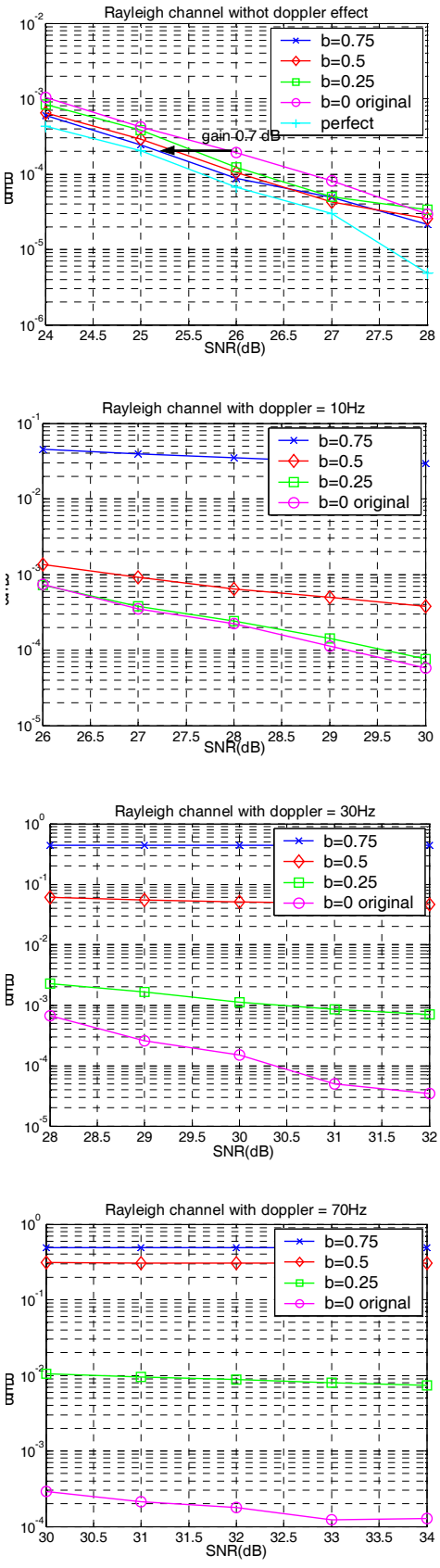

Fig. 20: simulation in Rayleigh channel with different Doppler effects

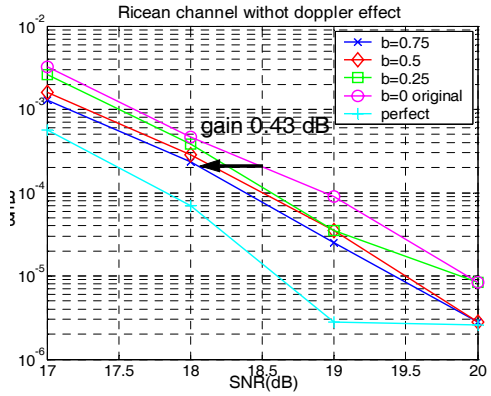

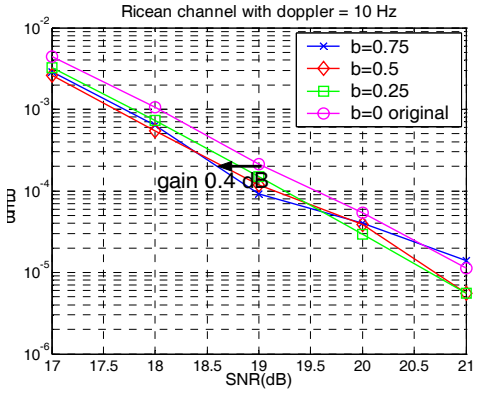

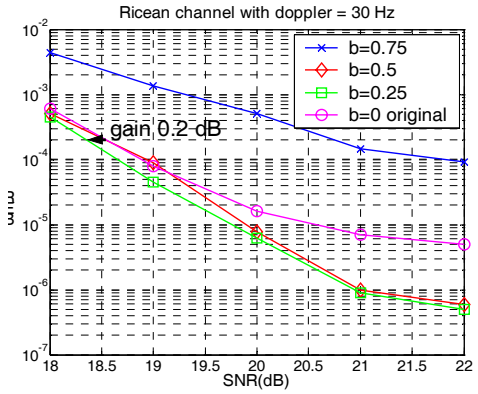

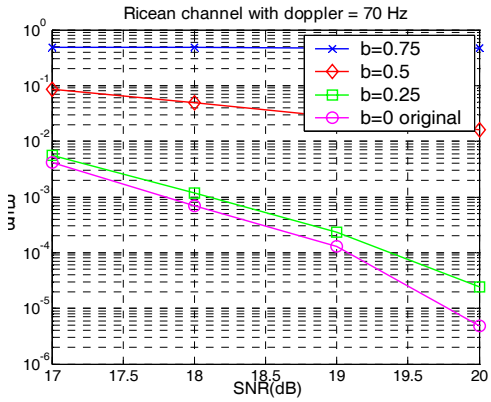

Fig. 21: simulation in Ricean channel with different Doppler effects

2. Filtering method

In fact, the CFR would be a smooth curve. According to this property, we use a low pass filter to reduce the high pass noise effect.

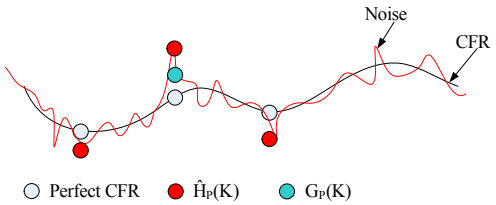

Fig. 22: The relationship of CFR and noise

In figure 22, we can see that the relationship of CFR and noise. Because of noise we can get the red circle CFR but the perfect CFR is white circle. So the basic concept of filtering is to get a smoother CFR (blue circle) by a LPF. In theory the blue circle $G_P(k)$ will be closer to perfect CFR than red circle $H_P(k)$.

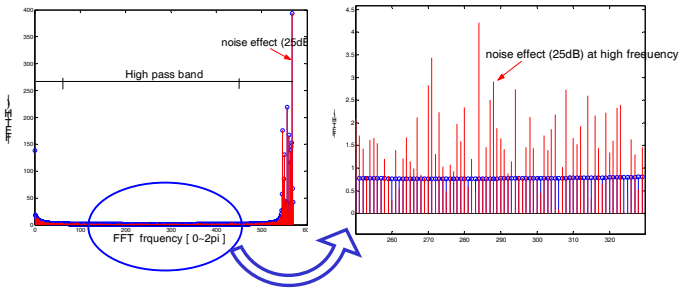

Fig. 23: The CFR of Rayleigh channel @ AWGN 25dB

In filtering processing, first we let the CFR through a FFT transform. The blue signal is the perfect CFR through FFT transform. The red signal is the perfect CFR add noise @ 25dB. We can see that, the energy is gathered in low pass band. In figure 23 we can see the noise effect at high pass band. So we can reduce the noise in high pass band by a LPF.

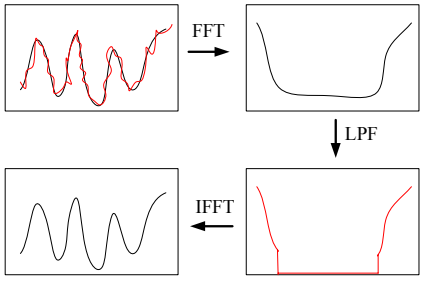

Fig. 24: The flow diagram

Fig. 24 is the filtering process flow diagrams. It contains M-point FFT/IFFT, and the cutoff-frequency of LPF is at 128 point. The performance will be shown in Fig. 25. In Fig 25, we can find the performance with filter get better almost 0.35dB than the design without filter.

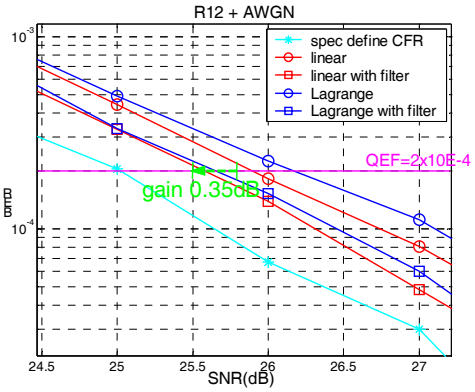

Fig. 25: performance in Rayleigh channel

3. Interpolation methods

In the above, we get the CFR at the pilot location. In this section, we propose the different interpolation methods to estimate the CFR of the whole symbol on data carrier locations. We adopted 2D interpolation method to estimate the CFR. First we do linear interpolation in time direction to defend the mobile environment. Here, we discuss the second interpolation in frequency direction. We will analyze some polynomial interpolation methods based on MSE and BER.

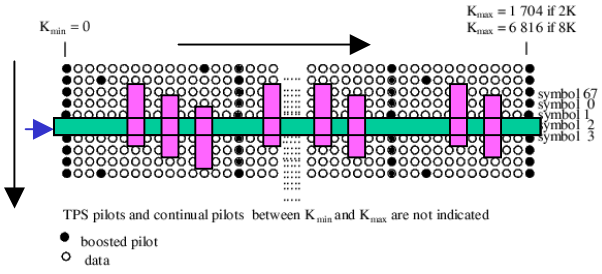

Fig. 26: The 2D interpolation

The formulation of CFR on data carrier is $\hat{H}(k) = \sum_j (\hat{H}(j) \times Cj)$. The basic concept is to get H(k) by adjacent points which CFR on pilots we estimate before. We will discuss the average, linear, Lagrange methods. And we will find high order interpolation can get better performance without noise.

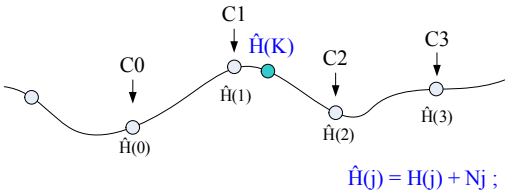

Fig. 27: The formulation of interpolation

The coefficients are listed on table 3. The algorithm of Lagrange is based on the formulation.

$$y(x) = \sum_{k=0}^{n} \frac{\pi(x)}{(x - x_k)\pi'(x_k)} f(x_k) = \sum_{k=0}^{n} l_k(x) f(x_k)$$

$$l_i(x) = \frac{(x - x_0)...(x - x_{i-1})(x - x_{i+1})...(x - x_n)}{(x_i - x_0)...(x_i - x_{i-1})(x_i - x_{i+1})...(x_i - x_n)}$$

Table 3: the coefficients list

	C0	C1	C2	C3
Average	0	0.5	0.5	0
Linear	0	0.3333	0.6666	0
Lagrange (2 order)	-0.1111	0.8889	0.2222	0
Lagrange (3 order)	-0.0617	0.7407	0.3704	-0.0494

The formulation detail is shown in following.

$$MSE = E\{|\hat{H} - H_k|^2\} = E\{|(\sum_j Cj \times (Hj + Nj)) - H_k|^2\}$$

$$= (\sum_j Cj^2)E[Nj^2] + \sum_j Cj^2 E[Hj^2] + \sum_{i \neq j} (2CiCj \times E[Hi]E[Hj]) + \sum_j (2Cj \times E[Hj]) \times H_k - H_k^2$$

The relationship of coefficients will make performance different. They are listed on Table3. We can find that the term $(\sum_j Cj^2)E[Nj^2]$ will be effected by noise directly. We find that it will enhance the noise effect with high order interpolation in comparison of $\sum_j (Cj^2)$.

In table 4, we can find the enhance term of each method. In AWGN only channel, the other term effect are all the same with each interpolation method. In this environment, we can find the average is better than linear and Lagrange in Fig. 28.

Table 4: the coefficients relationship

	Average	Linear	Lagrange (2 order)	Lagrange (3 order)
$\sum_j (Cj^2)$	0.5	0.5555	0.8519	0.6921
$\sum_{i \neq j} 2CiCj$	0.5	0.4444	0.1481	0.3078
$\sum_j 2Cj$	2.0	2.0	2.0	2.0

However, we care about the performance in Rayleigh channel. In the formulation, the other term effect will be different in each interpolation method. In fact the

CFR would be a smooth curve, so the higher order can get better performance in this effect.

$$\sum_j Cj^2 E[Hj^2] + \sum_{i \neq j} (2CiCj \times E[Hi]E[Hj]) + \sum_j (2Cj \times E[Hj]) \times H_k$$

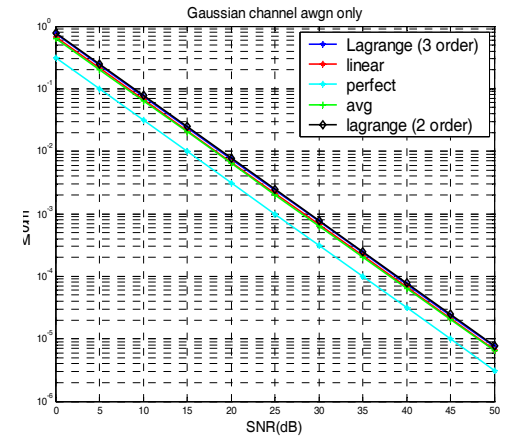

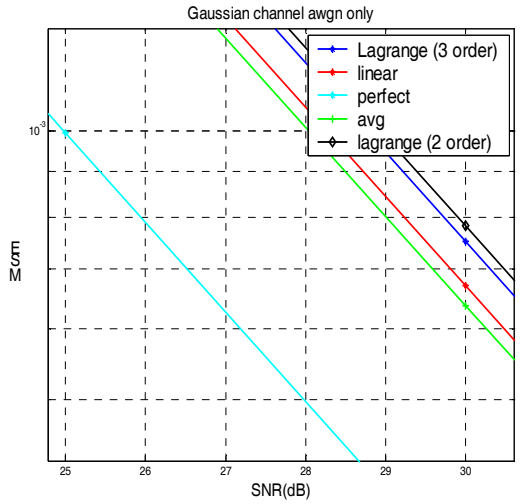

Fig. 28: AVG > Linear > Lagrange (3) > Lagrange (2) @all SNR @ Gaussian channel

The noise effect term $(\sum_j Cj^2)E[Nj^2]$ will be worse with higher order interpolation. So there will be a crossover in simulation with different SNR noise. The noise term will be dominant at low SNR, but the other term effect will be dominant at high SNR. The performance is shown in Fig. 29. In Fig 29 (a), we can find the crossover between linear curve and Lagrange curve is almost at SNR=35dB. In Fig. 29(b)(c), we can find linear will be better than Lagrange at low SNR, and Lagrange will be better than linear at high SNR. However, the QEF is almost at 25dB, so it is in low SNR range. So here we will adopt linear interpolation in frequency direction.

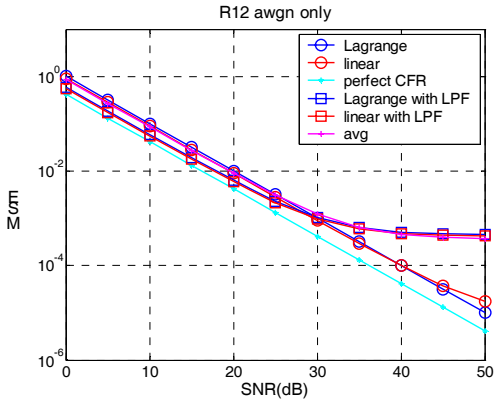

Fig 29(a): In Rayleigh channel, the QEF @ SNR=25dB

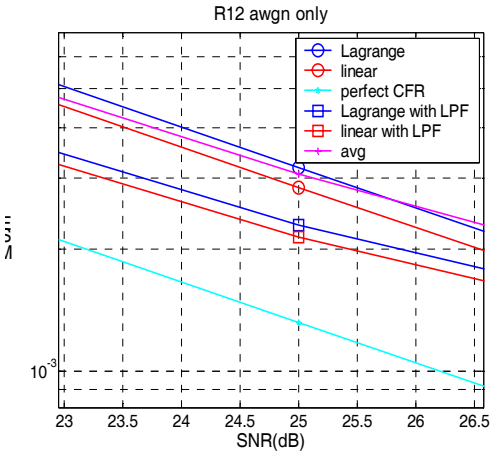

Fig. 29(b): @Low SNR right Linear>Lagrange

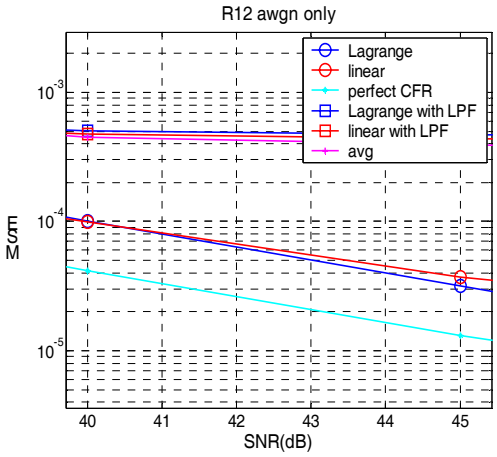

Fig.29(c): @ High SNR Lagrange>Linear

III. Conclusions

There are three parts mentioned above in channel estimation section. Each part is independent. So they can

work individually depend on the request. The motivation of the three parts is to get better performance to defend noise effect, but the method is focus on different aspects. Totally, it seems can gain about 0.5 dB to 1dB under slow fading channel.

Reference

[1] ETSI EN 300 744 v1.5.1, "Digital Video Broadcasting (DVB); Framing structure, channel coding and modulation for digital terrestrial television", Nov. 2004.

[2] ETSI EN 301 192 v1.4.1, "Digital Video Broadcasting (DVB); DVB specification for data broadcasting", May 2003.

[3] Cheng-Wei Kuang, "Timing Synchronization for DVB-T System", master thesis, Dep. of EE, NCTU, Taiwan, July 2004.

[4] Lei-Fone Chen, Yuan Chen, Lu-Chung Chien, Ying-Hao Ma, Chia-Hao Lee, Yu-Wei Lin, Chien-Ching Lin, Hsuan-Yu liu, Terng-Yin Hsu, Chen-Yi Lee, "A 1.8V 250mW COFDM Baseband Receiver for DVB-T/H Applications", in Proc. IEEE ISSCC2006, Feb. 2006.

[5] M. Speth, S. Fechtel, G. Fock and H. Meyr, "Optimum Receiver Design for OFDM-Based Broadband Transmission-Part II: A Case Study", IEEE Trans. Commun., vol. 49, No. 4, Apr. 2001

[6] DVB team of SI2 group, "The DVB project training documents", Dep. of EE, NCTU, Taiwan, July 2004.

[7] S. Liu and J. Chong, "A Study of Joint Tracking Algorithms of Carrier Frequency Offset and Sampling Clock Offset for OFDM-based WLANs", IEEE International Conf. Communications, Circuits and Systems and West Sino Expositions, vol. 1, July. 2002.

[8] P. Hoeher, S. Kaiser, and P. Robertson, "Two dimensional pilot-symbol-aided channel estimation by Wiener filtering", in Proc. IEEE ICSASSP'97, Munich, Germany, pp. 1845-4848, Apr. 1997

[9] F.B. Hildebrand, "introduction to numerical analysis" New York:McGraw-Hill,1956, Section 2.5

[10] M. Han Hsieh, C. H. Wei, "Channel Estimation for OFDM systems based on comb-type pilot arrangement in frequency selective fading channels", IEEE Trans. Consumer Electronics, Feb.1998

[11] Y. Zhao, A. Huang, "A Novel Channel Estimation Method for OFDM mobile communication systems based on pilot signal and transform-domain processing", in Proc. IEEE Vehicular Technology Conf., May. 1997

[12] L. Erup F. M. Gardner and R. A. Harris, "interpolation in digital Modems-Part II: implementation and performance", IEEE Trans. Commun., vol. 41, No. 6, Jun. 1993

[13] M. Sandell and O. Edfors, "A Comparative Study of Pilot-Based- Channel Estimators for Wireless OFDM", Research Report TULEA 1996